A Contribution to the Understanding of Carbonyl Migration in $Mn_2(CO)_{10}$ via the Pairwise Exchange Mechanism

Stephen A. Decker,† Oreola Donini, and Mariusz Klobukowski*

Department of Chemistry, University of Alberta, Edmonton, AB, T6G 2G2, Canada

Received: July 18, 1997[⊗]

Density functional theory using flexible Gaussian basis sets was employed in an all-electron ab initio study of $Mn_2(CO)_{10}$ that focused on the origins of the absence of carbonyl fluxionality in this compound. Calculations predict a staggered arrangement of carbonyls (D_{4d} symmetry) to be the most stable conformation of $Mn_2(CO)_{10}$, in agreement with experiment. Carbonyl migration then proceeds from the staggered conformer via rotation about the Mn−Mn bond to an eclipsed (D_{4h}) conformer, with a barrier of only 5 kcal/mol, and then to a symmetrical di-bridged (D_{2h}) conformer, through an additional barrier of 14−15 kcal/mol, and finally back to the staggered through the eclipsed conformer. The eclipsed conformer was found to be a transition state connecting two staggered conformers in the rotation about the Mn−Mn bond. The present estimate of 5 kcal/mol for the Mn−Mn rotation barrier is much lower than the previously reported value of 34 kcal/mol, and eliminates the rotational barrier as the sole origin of the absence of carbonyl migration in $Mn_2(CO)_{10}$. The present estimate of 19−21 kcal/mol for the overall activation energy for carbonyl scrambling in $Mn_2(CO)_{10}$ is fairly close to the upper limit of 25 kcal/mol for processes which may be followed using NMR spectroscopy.

Introduction

Ever since its discovery in the mid 1950s by Wilkinson and Piper,[1] ligand fluxionality in transition metal complexes has been a major area of interest in inorganic chemistry. Ligand migration is quite universal and has been observed in a variety of inorganic systems ranging from mononuclear complexes to multicenter metal clusters.[2,3]

The conventional experimental means of studying the dynamic fluxionality of ligands is NMR spectroscopy. This detection scheme does, however, place some limitations on the process to be studied. If the exchange process is to be detected by NMR, its rate must fall within the range $10^{-1}-10^{6}$ s^{-1}. Furthermore, the solvents employed restrict the range of temperatures at which the process can be followed, thereby imposing limitations on the activation energy. Generally, these dynamic processes must have an activation energy which falls within 3−25 kcal/mol in order for the process to be studied by NMR.[2]

Migration of the carbonyl group is the most common ligand exchange process studied, and it has been observed in a large number of transition metal clusters of varying nuclearity. Dimer complexes, due to their relative simplicity, are perhaps the best models to study, both experimentally and certainly theoretically, to elucidate all of the intricate mechanistic details of a ligand exchange process. Two mechanistic schemes were proposed and accepted for carbonyl scrambling in binuclear complexes: pairwise exchange and one-for-one exchange. In the pairwise exchange mechanism, proposed by Adams and Cotton[4] in the early 1970s, two of the migrating ligands are mutually exchanged between the two metal atoms. Symmetrical ligand bridges are opened and closed pairwise in a trans, coplanar, concerted fashion. This is the most common mechanism proposed for carbonyl migration and may proceed from an initial all-terminal or symmetrically bridging ground state. In the one-for-one mechanism, proposed by Evans et al.[5] for carbonyl exchange in *trans*-$(\eta^5\text{-}C_5H_5)_2Rh_2(CO)_3$ and $(\eta^5\text{-}C_5H_5)_2Rh_2(CO)_2P(OC_6H_5)_3$, the migrating ligands are not coplanar and are exchanged unsymmetrically in a stepwise fashion.

While transition metal carbonyls have been the focus of several theoretical studies, as illustrated in the recent papers by Ziegler et al.[6] and by Frenking et al.,[7] the analysis of carbonyl fluxionality in transition metal complexes is uncommon. One particularly interesting set of systems, in terms of their fluxional behavior, are the two Mn dimers, $Mn_2(CO)_{10}$, and $Mn_2(CO)_6(dppm)_2$, where dppm denotes bis(diphenylphosphino)methane. ^{13}C and ^{17}O NMR studies have shown[8] that the carbonyl ligands in $Mn_2(CO)_{10}$ remain fixed up to a temperature of 130 °C. However, when four of the carbonyls are replaced with two bidentate dppm ligands, then carbonyl fluxionality is observed, both by ^{13}C and ^{31}P NMR, down to a temperature as low as −75 °C.[9]

The $Mn_2(CO)_{10}$ dimer has been the subject of several computational studies; however, none of them focused on the dynamic fluxionality, or lack thereof, of the carbonyl ligands. Many of these studies have focused on the unique structural features of $Mn_2(CO)_{10}$. Electron diffraction studies, both in the gas phase[10] and in crystal[11,12] show that it has one of the longest metal−metal bonds known, about 2.9 Å, and the structure exhibits a characteristic bending of the four equatorial carbonyls toward the Mn atom to which they are not directly bound. Veillard et al.[13] probed the electronic and geometric structure of $Mn_2(CO)_{10}$, using ab initio RHF and CISD methods. Bo et al.[14] used the RHF ground-state wave function of $Mn_2(CO)_{10}$ in topological studies of electron density aimed at analyzing the Mn−Mn bond order. Nakatsuji et al.[15] also studied the nature of the Mn−Mn bond at the ab initio RHF level, both through the evaluation of potential energy curves and via the analysis of electron density difference maps. Recently, Baerends et al.[16] analyzed the effects of basis set variation on the Mn−Mn bond in $Mn_2(CO)_{10}$. Other papers have focused on the rich photochemistry of $Mn_2(CO)_{10}$. Two different photochemical reactions have been observed experimentally in the electronic absorption spectrum of $Mn_2(CO)_{10}$. One photoabsorption

† Harry Emmett Gunning Graduate Fellow 1994−96.

⊗ Abstract published in *Advance ACS Abstracts,* October 15, 1997.

S1089-5639(97)02355-4 CCC: $14.00 © 1997 American Chemical Society

TABLE 1: Basis Set Convergence Analysis for the Total Energy of CO at $R = 2.132$ a_o[a]

	convergence of total energy[b]			
basis set	$\Delta(SCF)$	$\Delta(MP2)$	$\Delta(CISD)$	$\Delta(DFT)$
	Convergence in d Space			
A1d−A[c]	66.0	145.6	147.9	44.0
A2d−A1d	5.1	25.5	22.9	3.1
A3d−A2d	1.1	5.2	4.3	0.9
A4d−A3d	0.1	2.1	2.0	0.1
A5d−A4d	0.2	0.7	0.6	0.3
	Convergence in f Space			
A3d1f−A3d	2.9	28.1	25.8	2.3
A3d2f−A3d1f	0.3	6.2	5.0	0.3
A3d3f−A3d2f	0.1	2.8	2.2	0.2
	Convergence in *g* Space			
A3d2f1g−A3d2f	0.3	9.3	7.7	0.2

[a] All values are in mE_h, with 1 $mE_h \approx 0.6$ kcal/mol. (Chemical accuracy is 1 kcal/mol.) [b] The lowering of the total energy is defined as $\Delta = E$(smaller basis) − E(larger basis). The reference energies in the unpolarized basis set *A* are (in hartree): $E(SCF) = -112.709867$, $E(MP2) = -112.945712$, $E(CISD) = -112.926711$, $E(DFT) = -113.300418$. In the MP2 and CISD calculations the two lowest molecular orbitals (corresponding to the 1s orbitals of carbon and oxygen) were frozen. [c] Basis A = Huzinaga's (10s6p)/[6s4p].[28] Exponents of polarization functions taken from Ahlrichs *et al*.[27b]

process leads to the dissociation of the Mn−Mn bond into two $Mn(CO)_5$ radicals, while the other leads to the dissociation of a carbonyl ligand. The papers of Levenson and Grey,[17] based on extended Hückel calculations, Márquez et al.,[18] based on ab initio RHF calculations, and Rosa et al.,[19] based on local DFT calculations, have all focused on this aspect of the chemistry of $Mn_2(CO)_{10}$. A previous theoretical study which is perhaps the most relevant to the problem of carbonyl scrambling was that of Folga and Ziegler[20] who calculated the energy barrier for rotation about the Mn−Mn bond, going from the staggered (D_{4d}) ground state conformation to the eclipsed (D_{4h}) conformation, using nonlocal DFT methodology with the BP86 functional.[21,22]

Numerous theoretical papers (see the recent reviews by Salahub and Zerner[23] and by Veillard[24]) have shown that electron correlation effects are very important in describing the bonding in transition metal complexes. Inclusion of electron correlation requires the use of either correlated wave function theory (WFT) methods,[25] such as Møller−Plesset perturbation methods (MP2, MP3 etc.), configuration interaction schemes (CISD, CISD(T) etc.), and multiconfigurational SCF or the density functional theory (DFT) methodologies.[26] Aside from decreased computational expense and increased facility of inclusion of electron correlation, the DFT methods also exhibit much faster basis set convergence than correlated WFT methods. Table 1 illustrates the convergence of the total energy of the CO molecule, calculated at the equilibrium internuclear distance of 2.132 a_o as a function of the polarization space. The calculations were done in the course of the present work, forming an extension of the study of Jankowski et al.[27] The convergence of DFT energy is similar to that of HF-SCF; both DFT and HF-SCF energies appear to be converged at the 2d1f level, while the correlated WFT methods (MP2 and CISD) remain unconverged even at the 3d2f1g level. This indicates that larger basis sets, with a more extensive complement of polarization functions that must include functions with a higher angular momentum quantum number, are required for correlated WFT methods than for DFT methods. It is a drawback of the DFT methods that the choice of functional is not straightforward, and its improvement is cumbersome. Nevertheless, for calculations involving relatively large transition metal complexes, in which a practical modest sized basis set must be employed, DFT used with nonlocal (gradient-corrected) functionals has become the method of choice, and has been very successful,[23] especially in the studies of bonding in transition metal complexes in their ground electronic states. It may be added that the utility of density functional theory in calculations of the excited states of molecules has not yet been fully exploited.[19,29]

In the present work, density functional theory was employed in an attempt to simulate the carbonyl fluxional behavior in $Mn_2(CO)_{10}$. On the assumption that carbonyl scrambling proceeds via the planar, pairwise exchange (merry-go-round) mechanism, the process was simulated by obtaining optimized geometries, frequencies, and energies of the conformers which play an integral role in the scheme. This allowed us to elucidate the mechanistic details for the scrambling process in $Mn_2(CO)_{10}$.

Along with the DFT calculations which employed nonlocal exchange and correlation functionals, HF-SCF calculations were performed in order to illustrate the importance of electron correlation in the systems. In addition, semiempirical calculations were used in order to gauge their ability to describe these relatively large metal-containing systems.

Computational Methods

The same all-electron basis set was used in the HF-SCF and DFT computations. This Gaussian basis set was of triple-ζ-valence quality, with double polarization (both p polarization functions), for the Mn atom, (533111/531*1*/311), and of double-ζ quality with one d polarization function for the C and O atoms, (421/31/1*). All basis sets were taken from our compilation.[30] The addition of an f-type polarization function to the Mn basis set was found by Baerends et al.[16] to have no significant effects, and such functions were not used in the present work. The final molecular basis set consisted of 346 contracted spherical Gaussian type functions for the $Mn_2(CO)_{10}$ conformers.

In the DFT calculations, the nonlocal (gradient corrected) exchange functional of Becke[21] was used together with the nonlocal correlation functional of Lee, Yang, and Parr.[31] (This combination is commonly referred to as the BLYP functional.) This functional has proven to yield reliable geometries and frequencies in a number of studies of transition metal carbonyls.[32] The necessity of the inclusion of nonlocal corrections to the exchange and correlational functionals in order to properly describe the synergistic metal−ligand bonding, through σ donation and π back-donation, in transition metal complexes has been reported in a number of papers.[32,33] Additional calculations were made using Becke's three-parameter hybrid functional[34] (B3LYP functional).

The semiempirical calculations utilized the unpublished PM3-tm set of parameters (called here PM3), as contained within the Spartan program.[35] The choice of the semiempirical method was based solely on the availability of parameters for Mn.

All geometries were fully optimized using analytical gradient techniques, and the nature of the resulting stationary point was characterized by harmonic vibrational analysis. To gain insight into the carbonyl scrambling mechanism, one must know not only the structures and relative energies of the species involved but also what, in chemical terms, the species correspond to. The energy Hessian was computed either using analytical second derivatives or via numerical evaluation of analytical first derivatives. The importance of analyzing the Hessian at a stationary point cannot be underestimated.

The HF-SCF and DFT calculations were carried out using the HONDO,[36] Gaussian 92/DFT,[37] and Gaussian 94[38] pro-

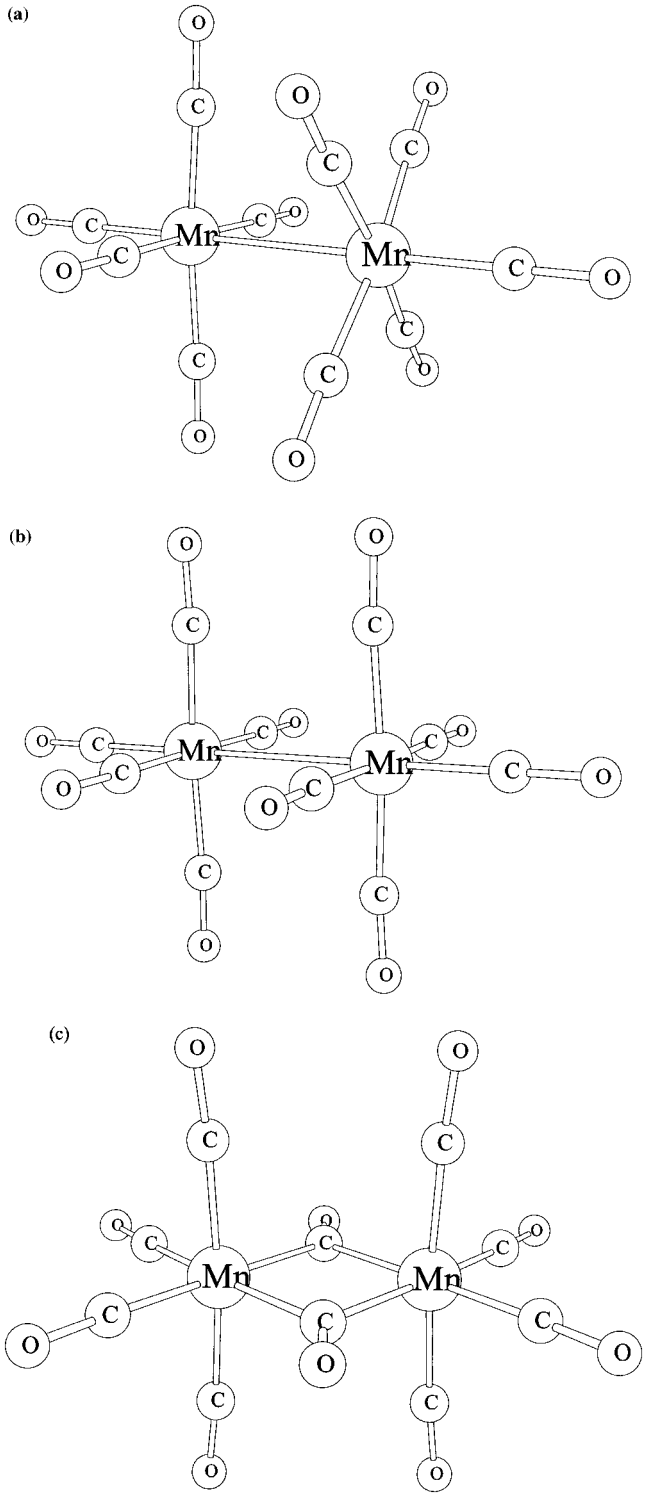

Figure 1. The three conformers of $Mn_2(CO)_{10}$ studied: (a) staggered, D_{4d}; (b) eclipsed, D_{4h}; (c) bridged, D_{2h}.

grams; the semiempirical calculations were done using the Spartan[35] package.

Results and Discussion

The structures of the staggered (D_{4d}), eclipsed (D_{4h}), and bridged (D_{2h}) conformers of $Mn_2(CO)_{10}$ are shown in Figure 1, and the optimized geometrical parameters are presented in Table 2, along with experimental values for the D_{4d} conformer and previous computational results for the D_{4d} and D_{4h} conformers. The following naming convention has been adopted to distinguish between the different carbonyl ligands in the three $Mn_2(CO)_{10}$ conformers. In the staggered (D_{4d}) and eclipsed (D_{4h}) conformers the axial carbonyls are defined to be collinear to the Mn−Mn bond, and the remaining eight carbonyls are labeled as equatorial. In the bridged (D_{2h}) conformer, "terminal" is used to label the four carbonyls coplanar with the two bridging carbonyls, and "perpendicular" labels the remaining four carbonyls.

Comparison of the calculated and experimental geometries of the D_{4d} conformation convincingly shows the shortcomings of the HF-SCF methodology. HF-SCF overestimates the Mn−Mn and Mn−C bond distances by as much as 0.3 Å. The calculated C−O distances are slightly underestimated, although it is hard to make any strict comparison here as the gas-phase diffraction data represent averaged values. Overall, the HF-SCF optimized geometry shows an average deviation of 0.15 Å (and a maximum deviation of 0.32 Å) in bond lengths when compared to the gas-phase diffraction geometry (expt A) for the D_{4d} conformer. The bond angles were predicted with slightly better accuracy having an average deviation of 1.8° (with a maximum deviation of 1.9°). Clearly, the ab initio HF-SCF method is unable to correctly describe the single metal−metal bond in $Mn_2(CO)_{10}$.

The geometry of the D_{4d} conformer optimized using nonlocal DFT is much closer to the experimentally observed structure than that predicted by HF-SCF theory. DFT-BLYP predicts the Mn−Mn bond to be nearly identical with its gas-phase diffraction value, while the Mn−C and C−O distances appear to be very slightly overestimated. The average deviations (maximum deviations given in parentheses) of the calculated and experimental bond distances and bond angles are 0.01 Å (0.02 Å) and 0.3° (0.6°), respectively. Comparison of the present DFT results (obtained with the nonlocal BLYP functional) with the previous DFT results obtained by Folga and Ziegler[20] (nonlocal BP86 functional) and Rosa et al.[19] (local density functional) indicates that the BLYP functional predicts geometries which are, not surprisingly, much more accurate than the local functional and as accurate as the BP86 functional. However, a direct comparison of functionals is of limited value as different basis sets were used in different calculations.

Surprisingly, the D_{4d} geometry predicted by the semiempirical PM3 method is in reasonable agreement with experiment, even though the PM3 parametrization leads to Mn−Mn and Mn−C distances that are too short and overestimates the C−O distances. The average (and maximum) deviations of the predicted and observed experimental bond distances and angles are 0.03 Å (0.06 Å) and 1.2° (2.0°), respectively. The PM3 method therefore predicts geometries that have a much higher accuracy than the HF-SCF and local DFT methods, but inferior to the accuracy of the nonlocal DFT methods.

Differences in bond lengths may provide insight into the nature of bonding between the atoms involved. For example, a shorter Mn−C distance indicates a stronger bond while a longer C−O distance indicates that the Mn−C bond was strengthened by increasing the electronic population of the CO π^* antibonding orbitals via Mn→CO π back-donation. It must be mentioned here that the experimental data are of limited use, as the experimental geometries differ substantially, perhaps due to different experimental conditions (gas-phase diffraction vs crystal structure diffraction experiment, or crystal structure determinations carried out at different temperatures). The HF-SCF calculations predict shorter $Mn-C_{ax}$ bonds and shorter $C_{ax}-O_{ax}$ bonds. Both the DFT-BLYP and PM3 calculations predict stronger bonding of the axial carbonyls to Mn (through increased π back-donation) than that of the equatorial carbonyls.

TABLE 2: Predicted Geometrical Parameters for the Three Conformers of $Mn_2(Co)_{10}$[a]

		this work			experiment			previous DFT	
conformer	parameter	SCF	DFT	PM3[b]	A[c]	B[d]	C[e]	Ziegler[f]	Rosa[g]
Staggered D_{4d}	Mn−Mn	3.298	2.979	2.919	2.977	2.895	2.923	2.902	2.876
	$Mn-C_{ax}$	2.006	1.827	1.788	1.803	1.820	1.792	1.813	1.747
	$Mn-C_{eq}$	2.028	1.874	1.852	1.873	1.859	1.831	1.859	1.799
	$C_{ax}-O_{ax}$	1.111	1.165	1.168	1.147[h]	1.150	1.151	1.158	1.172
	$C_{eq}-O_{eq}$	1.116	1.162	1.161	1.147[h]	1.140	1.157	1.153	1.169
	$C_{eq}-Mn-Mn$	84.2	86.6	86.8	86.1	86.3	87.0	85	
	$O_{eq}-C_{eq}-Mn$	176.1	177.2	179.8		177.8	177.3	175.9	
	$C_{eq}-Mn-C_{ax}$	95.8	93.4	93.1	93.4	93.9	93.8	93.0	
Eclipsed D_{4h}	Mn−Mn	3.518	3.116	2.966				2.965	
	$Mn-C_{ax}$	2.014	1.823	1.789				1.812	
	$Mn-C_{eq}$	2.031	1.874	1.851				1.850	
	$C_{ax}-O_{ax}$	1.111	1.165	1.169				1.157	
	$C_{eq}-O_{eq}$	1.116	1.162	1.161				1.156	
	$C_{eq}-Mn-Mn$	85.5	87.5	88.7				89.1	
	$O_{eq}-C_{eq}-Mn$	178.5	175.3	176.2				174.4	
	$C_{eq}-Mn-C_{ax}$	94.5	92.5	91.3				90.9	
Bridged D_{2h}	Mn−Mn	3.062	2.846						
	$Mn-C_{perp}$	2.042	1.871						
	$Mn-C_{term}$	1.994	1.853						
	$Mn-C_{br}$	2.214	2.109						
	$C_{perp}-O_{perp}$	1.112	1.160						
	$C_{term}-O_{term}$	1.112	1.160						
	$C_{br}-O_{br}$	1.153	1.183						
	$C_{term}-Mn-Mn$	131.32	130.30						
	$O_{term}-C_{term}-Mn$	175.96	176.61						
	$C_{term}-Mn-C_{perp}$	89.92	88.28						

[a] Bond lengths in angstroms, angles in deg. [b] A limitation of the Spartan program package and unavailability of the source code prevented selection of the correct electronic configuration in the D_{2h} conformer and made the study of the bridged structure impossible. [c] Gas-phase electron diffraction study at room temperature.[10] [d] Electron diffraction crystal structure at 74 K.[11] [e] Electron diffraction crystal structure at room temperature.[12] [f] DFT study[20] using nonlocal exchange and correlation functionals (the BP86 functional[21,22]). [g] DFT study[19a] using a local spin density functional (the VWN functional). [h] Averaged distances.

Rotation about the Mn−Mn bond to make six carbonyls coplanar, a necessary step if carbonyl scrambling in $Mn_2(CO)_{10}$ is to proceed via a pairwise exchange scheme, induces large changes in the bond distances and angles from their values in the staggered conformation, as shown in Table 2. The present calculations, as well as those done by Folga and Ziegler,[20] predict, as expected on the basis of simple steric or electrostatic arguments, that rotation about the Mn−Mn bond to the eclipsed conformation causes a large increase in the Mn−Mn distance. The HF-SCF calculations predict an increase of 0.22 Å, leading to an incredibly long Mn−Mn bond of over 3.5 Å. The DFT-BLYP calculations predict a lengthening of the Mn−Mn bond by 0.04 Å, while Ziegler's DFT-BP86 calculations predict a lengthening of about 0.06 Å. The Mn−Mn distance is predicted to be 2.966 Å by the PM3 method, increased by 0.05 Å from its value in the staggered conformation. Interestingly, regardless of the computational method used, the rotation about the Mn−Mn bond has only a slight effect on the Mn−C and C−O distances and the bond angles.

The next step in the simulation of the merry-go-round mechanism is the formation of the eclipsed, symmetrical di-bridging (D_{2h}) conformer. The geometry of the bridged D_{2h} conformer was successfully optimized in the HF-SCF and DFT-BLYP calculations, and the results are shown in Table 2. The Mn−Mn bond length is drastically reduced in going from the eclipsed D_{4h} conformer to the bridged D_{2h} conformer. The formation of the bridged D_{2h} conformer from the eclipsed D_{4h} conformer, due to the bridging role of the two μ_2 carbonyls, reduces the Mn−Mn distance by 0.46 and 0.27 Å in the HF-SCF and DFT calculations, respectively. The Mn−C distances of the terminal, coplanar carbonyls of the bridged dimer are predicted to be shorter than the equatorial carbonyls in both the D_{4d} and D_{4h} conformers, while the Mn−C distance of the carbonyls perpendicular to the plane containing the bridged carbonyls (labeled as C_{perp} in Table 2) are predicted to be longer than both sets of nonequivalent Mn−C distances (axial and equatorial carbonyls) in the D_{4d} and D_{4h} conformers. HF-SCF and DFT-BLYP both predict the following trend for the Mn−C distances of the bridged D_{2h} conformer: $Mn-C_{br} > Mn-C_{perp} > Mn-C_{term}$.

TABLE 3: Relative Energies of the $Mn_2(Co)_{10}$ Conformers

conformer	method	relative energy[a]
eclipsed (D_{4h})	HF-SCF	5.3
	DFT-BLYP	4.8
	DFT-BP86[b]	34.0
	PM3	10.8
bridged (D_{2h})	HF-SCF	52.2
	DFT-BLYP	18.6

[a] In kcal/mol, with respect to the staggered (D_{4d}) conformer. The reference total energies are: E(HF-SCF) = −3424.87128E_h, E(DFT-BLYP) = −3433.75626 E_h, ΔH_f° (PM3) = −698.7 kcal/mol. Note: same basis set used in both HF SCF and DFT calculations. [b] Folga and Ziegler.[20]

The relative energies of the three conformers that were expected to play the central role in the carbonyl scrambling in $Mn_2(CO)_{10}$ are shown in Table 3. All three methods predict the D_{4d} staggered conformation to be the ground state for $Mn_2(CO)_{10}$. The D_{4h} eclipsed conformer is predicted by HF-SCF and DFT-BLYP to lie about 5 kcal/mol above the staggered conformer. The DFT-B3LYP value is slightly larger, 6 kcal/mol. PM3 predicts the energy gap to be twice as large. The BP86 value of the energy difference between these two conformers, calculated by Folga and Ziegler[20] to be 34 kcal/mol, is surprisingly large. The D_{2h} bridged conformer is predicted by DFT-BLYP to lie a further 14 kcal/mol above the eclipsed conformer, DFT-B3LYP finds it at 15 kcal/mol, while HF-SCF predicts it to lie much higher in energy, almost 47 kcal/mol above the eclipsed conformation. As stated earlier,

TABLE 4: IR-Active Normal Modes of Ground State D_{4d} $Mn_2(Co)_{10}$

HF[a]			DFT[a]			PM3[a]			expt A[b]			expt B[c]		
ω[d]	I[e]	deg[f]	ω[d]	I[e]	deg[f]	ω[d]	I[e]	deg[f]	ω[d]	I[e]	deg[f]	ω[d]	I[e]	deg[f]
2079	1.6	1	2055	2.2	1	2094	2.1	1	2053		1	2045	2.0	1
2028	5.6	2	2025	6.6	2	2038	7.3	2	2025		2	2014	7.0	2
1977	1.0	2	2003	1.0	1	1962	1.0	1	1992		1	1983	1.0	1
472	0.2	2	664	0.9	1	672	1.6	2						
459	0.3	1	660	0.5	2	655	1.5	1						

[a] Calculated frequencies were corrected using the scaling factors of 0.87, 1.02, and 0.98 for the HF-SCF, DFT-BLYP, and PM3 values, respectively. [b] Gas-phase IR experiment.[39] [c] IR spectrum in *n*-hexane.[40] [d] Frequencies in cm^{-1}. [e] Intensities in arbitrary units. [f] Degeneracy.

optimization of the bridged species using the PM3 method was unsuccessful.

At all three levels of theory the lowest energy, staggered, D_{4d} conformer of $Mn_2(CO)_{10}$ was found to be a minimum on the potential energy surface based on harmonic vibrational analysis. The calculated frequencies of the IR-active modes of the ground-state D_{4d} staggered conformer are reported in Table 4, along with the experimental C−O stretching frequencies. To obtain the smallest average deviations of the frequencies for the C−O stretches when compared to the experimental gas-phase values of Parker,[39] scaling factors of 0.87, 1.02, and 0.98 were applied to the calculated HF-SCF, DFT-BLYP, and PM3 frequencies. Once again, DFT yields the most accurate calculated values, not only with a correction factor very close to unity, but also with the smallest average deviation of the C−O stretching frequencies, 4 cm^{-1}, when compared to experiment. PM3, although having a correction factor which is as close to unity as DFT-BLYP, has a much larger deviation of 28 cm^{-1} when compared to experiment. HF-SCF, with a typical value of the scaling factor, still has an average deviation of 15 cm^{-1} for the corrected C−O stretching frequencies when compared to their experimental values. The relative intensities of the three C−O stretching bands mimic the experimental spectrum very well. The nuclear displacements in these three modes are shown in Figure 2. The two degenerate modes with frequency 2025 cm^{-1} correspond to combination of stretching vibrations of the equatorial carbonyls. The two other modes, at 2055 cm^{-1} and at 2003 cm^{-1} are combinations of stretches of all carbonyls.

The eclipsed conformer was found to be a genuine transition state at the HF-SCF and DFT-BLYP levels of theory, with imaginary harmonic frequencies of 33*i* cm^{-1} and 28*i* cm^{-1}, respectively. The analogous stationary point on the PM3 potential energy surface is a third-order saddle point, with harmonic frequencies of 47*i* and (twice) 30*i* cm^{-1}. Examination of the vibrational normal mode associated with the single negative eigenvalue of the Hessian matrix in the HF and DFT calculations, and the largest, most negative Hessian eigenvalue in the PM3 calculations, revealed that the eclipsed conformer is a transition state connecting two ground-state staggered conformers. The motions of the nuclei in this mode are shown in Figure 3.

The barrier to rotation about the Mn−Mn bond is fairly small, and hence the rotation should be rapid. Since the eclipsed conformer is a transition state for a simple rearrangement of one staggered conformation to another, via rotation about the Mn−Mn bond, it is possible to calculate a unimolecular rate constant for this process from the energies, zero-point corrections, and partition functions of the ground state and transition state. Utilizing the data from Table 5 and the simplified formalism of Maskill,[41] the rate constant was estimated at 1×10^8 s^{-1} and 6×10^8 s^{-1} from the HF and DFT data, respectively.

Due to the prohibitively long computational time of evaluating the Hessian with the DFT method, the Hessian of the bridged conformer was evaluated only using the HF-SCF method; at this level, the bridged species corresponds to a second-order

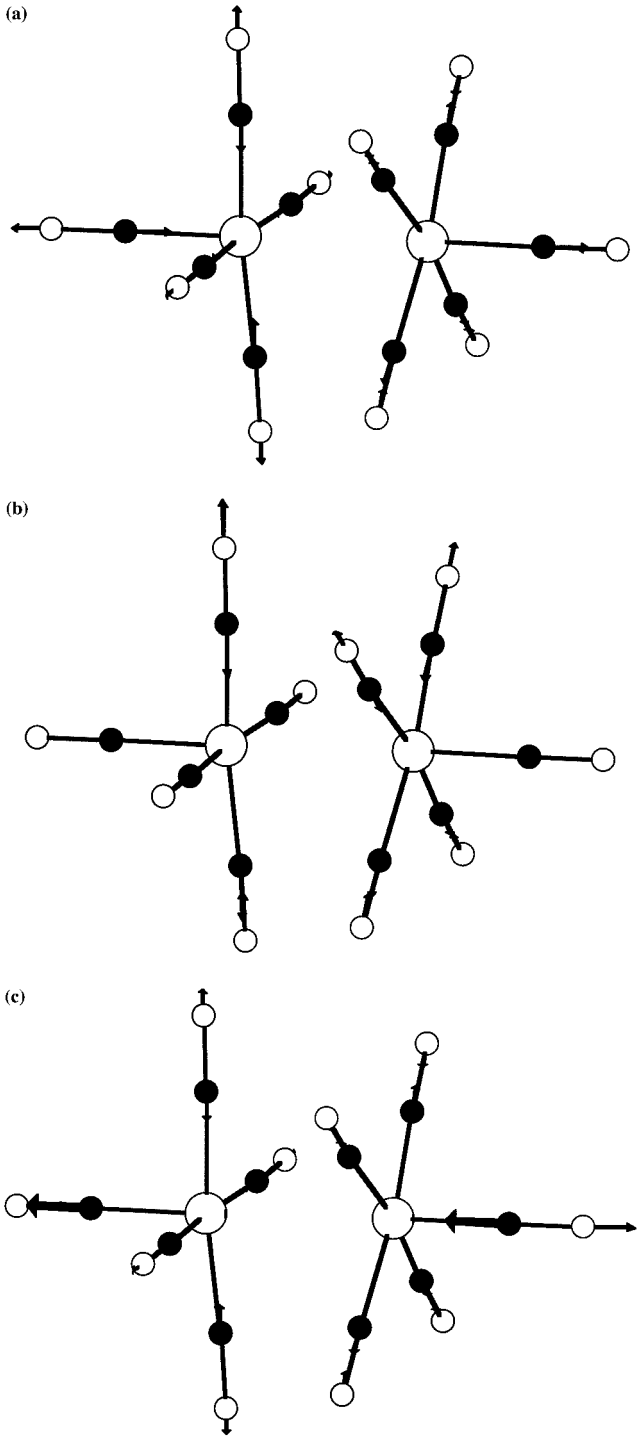

Figure 2. Motions of the nuclei in the carbonyl stretching vibrations in the staggered D_{4d} conformer: (a) 2055 cm^{-1}; (b) 2025 cm^{-1} (one of the two degenrate modes); (c) 2003 cm^{-1}.

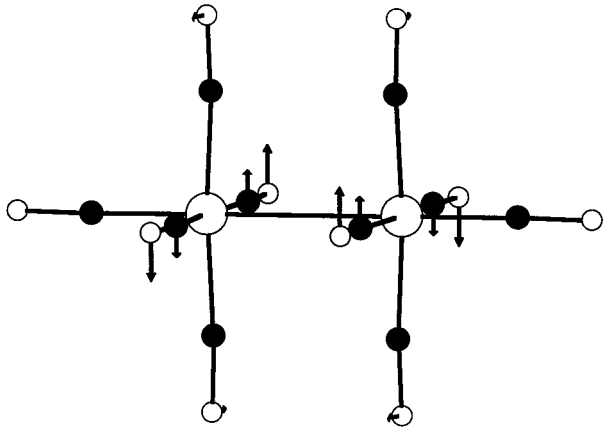

Figure 3. Motions of the nuclei in the harmonic mode corresponding to the single negative curvature of the HF-SCF and DFT potential energy surfaces in the D_{4h} transition state.

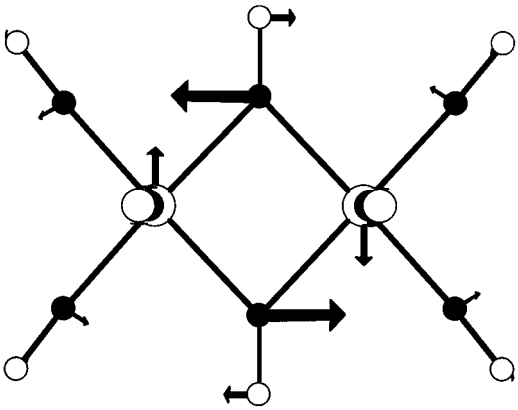

Figure 4. Motions of the nuclei in the harmonic vibrational mode connecting the bridged (D_{2h}) and eclipsed (D_{4h}) $Mn_2(CO)_{10}$ conformers.

TABLE 5: Data for the Determination of the Eclipsed-Staggered Unimolecular Rate Constant

conformer	method	E_{Tot}/E_h	ZPE/E_h	Q/10^{25}
eclipsed (D_{4h})	HF-SCF	−3424.86284	0.08497	6.52325
	DFT-BLYP	−3433.74854	0.08289	0.84008
staggered (D_{4d})	HF-SCF	−3424.87128	0.08499	39.3451
	DFT-BLYP	−3433.75626	0.08294	22.7862

saddle point with associated imaginary frequencies of 370*i* and 49*i* cm^{-1}. The 370*i* cm^{-1} vibrational normal mode, shown in Figure 4, corresponds to carbonyl scrambling via the pairwise exchange mechanism between what appears to be two eclipsed conformers.

Vibrational analysis of all conformers indicates that the potential energy surfaces near the stationary points are quite flat, leading to a large number of modes with small frequencies. For example, in the staggered conformer, there were 44, 38, and 34 vibrational modes (over half of all modes) with frequencies smaller than 500 cm^{-1}, as predicted by our HF, DFT, and PM3 calculations.

Conclusions

The results of the present nonlocal DFT calculations indicate that the merry-go-round carbonyl scrambling in $Mn_2(CO)_{10}$ proceeds from the most stable staggered D_{4d} conformation to the eclipsed D_{4h} conformation, with a barrier of 5 kcal/mol, to the bridged D_{2h} conformer, with a barrier of 14−15 kcal/mol, and then back via the eclipsed conformer to the staggered one. The D_{4d} conformer, corresponding to a local minimum on the potential energy surface, was characterized as a genuine chemical species. The D_{4h} conformer was found to be a transition state for the simple rearrangement from one staggered conformer to another. At the HF-SCF level, the D_{2h} conformer was found to be a second-order saddle point, with the largest negative curvature of the potential energy surface corresponding to the transition state for the merry-go-round carbonyl migration process connecting two D_{4h} conformers. The fluxional process induces substantial changes in the Mn−Mn and Mn−C distances and proceeds with an activation energy of 19−21 kcal/mol. This barrier for carbonyl fluxionality, calculated for the interconversion in the gas phase, is fairly close to the upper limit of 25 kcal/mol for processes in solution that may be followed by NMR spectroscopy.[2] The barrier for the rotation about the Mn−Mn bond, predicted to be only 5 kcal/mol, is much smaller than the value of 34 kcal/mol previously reported[20] and is more in accord with the single-bond character of the Mn−Mn bond. The rotation should be rapid, with an estimated rate constant of the order of 10^8 s^{-1}.

As expected, the single-determinant HF-SCF method was unsuccessful in modeling these large metal dimer systems, yielding poor geometries and a very large activation barrier for carbonyl migration in $Mn_2(CO)_{10}$. The central Mn−Mn bond appears to be very malleable at the HF-SCF level, responding with large changes to ligand rearrangement. The softness of this bond is further revealed in the harmonic vibrational frequency corresponding to the (IR-inactive) stretch of the Mn−Mn bond, which is only 481 cm^{-1} at the HF-SCF level; the DFT value is 686 cm^{-1}. The DFT methods with nonlocal exchange and correlation functionals performed much better in the prediction of both geometries and activation energies for the metal dimer studied. Surprisingly, the semiempirical PM3 method yields quite accurate molecular geometry for the most stable conformer, rivaling the accuracy of the more sophisticated nonlocal DFT calculations. However, the PM3 method may be less successful in predicting the activation energies.

Acknowledgment. This study was inspired by a lecture given by Professor Josef Takats at the University of Alberta. Subsequent discussions with Professor Takats are gratefully acknowledged. All calculations were done on the IBM RS/6000 workstations and on the IBM SP2 installation at the University of Alberta. This work was financed partly by a research grant from NSERC, and partly by the University of Alberta. S.A.D. would also like to thank the Faculty of Graduate Studies at the University of Alberta for a scholarship and to the Department of Chemistry for the Harry Emmett Gunning Graduate Fellowship.

References and Notes

(1) Wilkinson, G.; Piper, T. S. *J. Inorg. Nucl. Chem.* **1956**, *2*, 23.
(2) Band, E.; Muetterties, E. L. *Chem. Rev.* **1978**, *78*, 639.
(3) de Mayo, P., Ed. *Rearrangements in Ground and Excited States*; Academic: New York, 1980.
(4) Adams, R. D.; Cotton, F. A. *J. Am. Chem. Soc.* **1973**, *95*, 6589.
(5) (a) Evans, J.; Johnson, B. F. G.; Lewis, J.; Norton, J. R. *Chem. Commun.* **1973**, *73*, 79. (b) Evans, J.; Johnson, B. F. G.; Lewis, J.; Matheson, T. W. *Chem. Commun.* **1975**, *75*, 576.
(6) Li, J.; Schreckenbach, G.; Ziegler, T. *J. Am. Chem. Soc.* **1995**, *117*, 486.
(7) Ehlers, A. W.; Frenking, G. *Organometallics* **1995**, *14*, 423. Ehlers, A. W.; Dapprich, S.; Vyboishchikow, S. F.; Frenking, G. *Organometallics* **1996**, *15*, 105.
(8) (^{13}C) Todd, L. J.; Wilkinson, J. R. *J. Organomet. Chem.* **1974**, *77*, 1. (^{17}O) Aime, S.; Milone, L.; Osella, D.; Hawkes, G. E.; Randall, E. W. *J. Organomet. Chem.* **1979**, *178*, 171.
(9) Marsella, J. A.; Caulton, K. G. *Organometallics* **1982**, *1*, 274.
(10) Almenningen, A.; Jacobsen, G. G.; Seip, H. M. *Acta Chem. Scand.* **1969**, *23*, 685.
(11) Martin, M.; Rees, B.; Mitschler, A. *Acta Crystallogr.* **1982**, *B38*, 6.

(12) Dahl, L. F.; Rundle, R. E. *Acta Crystallogr.* **1963**, *16*, 419.
(13) Veillard, A.; Rohmer, M.-M. *Int. J. Quantum Chem.* **1992**, *42*, 965.
(14) Bo, C.; Sarasa, J.-P.; Poblet, J.-M. *J. Phys. Chem.* **1993**, *97*, 6362.
(15) Nakatsuji, H.; Hada, M.; Kawashima, A. *Inorg Chem.* **1992**, *31*, 1740.
(16) Rosa, A.; Ehlers, A. W.; Baerends, E. J.; Snijders, J. G.; te Velde, G. *J. Phys. Chem.* **1996**, *100*, 5690.
(17) Levenson, R. A.; Gray, H. B. *J. Am. Chem. Soc.* **1975**, *97*, 6042.
(18) Márquez, A.; Fernández Sanz, J.; Gelizé, M.; Dargelos, A. *J. Organomet. Chem.* **1992**, *434*, 235.
(19) (a) Rosa, A.; Ricciardi, G.; Baerends, E. J.; Stufkens, D. J. *Inorg Chem.* **1995**, *34*, 3425. (b) Rosa, A.; Ricciardi, G.; Baerends, E. J.; Stufkens, D. J. *Inorg. Chem.* **1996**, *35*, 2886.
(20) Folga, E.; Ziegler, T. *J. Am. Chem. Soc.* **1993**, *115*, 5169.
(21) Becke, A. *Phys. Rev. A* **1988**, *38*, 3098.
(22) Perdew, J. P. *Phys. Rev. B* **1986**, *33*, 8822.
(23) Salahub, D. R.; Zerner, M. C. The Challenge of d and f electrons; ACS Symposium Series No. 394, American Chemical Society: Washington, DC, 1989.
(24) Veillard, A. *Chem. Rev.* **1991**, *91*, 743.
(25) (a) Raghavachari, K.; Anderson, J. B. *J. Phys. Chem.* **1996**, *100*, 12960. (b) Head-Gordon, M. *J. Phys. Chem.* **1996**, *100*, 13213.
(26) Kohn, W.; Becke, A. D.; Parr, R. G. *J. Phys. Chem.* **1996**, *100*, 12974.
(27) (a) Jankowski, K.; Becherer, R.; Scharf, P.; Schiffer, H.; Ahlrichs, R. *J. Chem. Phys.* **1985**, *82*, 1413. (b) Ahlrichs, R.; Scharf, P.; Jankowski, K. *Chem. Phys.* **1985**, *98*, 381.
(28) Huzinaga, S. J. *Chem. Phys.* **1965**, *42*, 1293.
(29) Ziegler, T.; Rauk, A.; Baerends, E. J. *Theor. Chim. Acta* **1977**, *43*, 261.
(30) Huzinaga, S., Ed. *Gaussian Basis Sets for Molecular Calculations*; Elsevier: Amsterdam, 1984.
(31) Lee, C.; Yang, W.; Parr, R. G. *Phys. Rev. B* **1988**, *37*, 785.
(32) Delley, B.; Wrinn, M.; Luthi, H. P. *J. Chem. Phys.* **1994**, *100*, 5785.
(33) Fan, L; Ziegler, T. *J. Chem. Phys.* **1991**, *95*, 7401.
(34) Becke, A. *J. Chem. Phys.* **1993**, *98*, 5648.
(35) Spartan 4.0.3, Wavefunction, Inc., Irvine, CA 92715, 1995.
(36) HONDO 95.6: Dupuis, M.; Marquez, A.; Davidson, E. R.: IBM Corporation, Neighborhood Road, Kingston, NY 12401.
(37) GAUSSIAN 92/DFT, Revision F.2: Frisch, M. J.; Trucks, G. W.; Schlegel, H. B.; Gill, P. M. W.; Johnson, B. G.; Wong, M. W.; Foresman, J. B.; Robb, M. A.; Head-Gordon, M.; Replogle, E. S.; Gomperts, R.; Andres, J. L.; Raghavachari, K.; Binkley, J. S.; Gonzalez, C.; Martin, R. L.; Fox, D. J.; DeFrees, D. J.; Baker, J.; Stewart, J. J. P.; Pople, J. A.; Gaussian, Inc.: Pittsburgh, PA, 1993.
(38) GAUSSIAN 94, Revision D.3: Frisch, M. J.; Trucks, G. W.; Schlegel, H. B.; Gill, P. M. W.; Johnson, B. G.; Robb, M. A.; Cheeseman, J. R.; Keith, T.; Petersson, G. A.; Montgomery, J. A.; Raghavachari, K.; Al-Laham, M. A.; Zakrzewski, V. G.; Ortiz, J. V.; Foresman, J. B.; Cioslowski, J.; Stefanov, B. B.; Nanayakkara, A.; Challacombe, M.; Peng, C. Y.; Ayala, P. Y.; Chen, W.; Wong, M. W.; Andres, J. L.; Replogle, E. S.; Gomperts, R.; Martin, R. L.; Fox, D. J.; Binkley, J. S.; DeFrees, D. J.; Baker, J.; Stewart, J. P.; Head-Gordon, M.; Gonzalez, C.; Pople, J. A.; Gaussian, Inc.: Pittsburgh, PA, 1995.
(39) Parker, D. J. *Spectrochim. Acta* **1983**, *39A*, 463.
(40) Haas, H; Sheline, R. K. *J. Chem. Phys.* **1967**, *47*, 2996.
(41) Maskill, H. *The Physical Basis of Organic Chemistry*; Oxford University Press: Oxford, 1989.